Available online at www.sciencedirect.com

ScienceDirect

Procedia Engineering 167 (2016) 252 – 264

Procedia Engineering

www.elsevier.com/locate/procedia

THE EFFECT OF SLAMMING IMPACT ON OUT-OF-AUTOCLAVE CURED PREPREGS OF GFRP COMPOSITE PANELS FOR HULLS

J.C. Suárez*, P. Townsend, E. Sanz, I. Diez de Ulzurrum, P. Pinilla

Higher Technical School of Naval Architecture and Ocean Engineering Department, Technical University of Madrid, Spain.

Abstract

This paper proposes a methodology that employs an experimental apparatus that reproduces, in pre-impregnated and cured out-of-autoclave Glass Fiber Reinforced Polymer (GFRP) panels, the phenomenon of slamming or impact on the bottom of a high-speed boat during planing. The pressure limits in the simulation are defined by employing a finite element model (FEM) that evaluates the forces applied by the cam that hits the panels in the apparatus via microdeformations obtained in the simulation. The methodology requires that various impact series be performed at different energies and that the evolution of the damage be followed via immersion ultrasound inspection to quantify how the material behaves, in addition to evaluating the delamination process via penetrating dyes using UV radiation. Slamming impacts were performed on the order of 10^5, and the micromechanisms of interlaminar and intralaminar damage propagation were observed with scanning electron microscopy (SEM). The results were analyzed by correlating them with pressure, deformation, impact energy, and applied cycles, in addition to conducting compression experiments after impact to relate the material damage with the residual strength of the impacted panels.

Peer-review under responsibility of the Organizing Committee of DRaF2016

Keywords: slamming, GFRP, impact, damage

1. Introduction

The experimental method proposed makes it possible to determine the behavior of composite materials used in building speedboats that are subject to slamming phenomena by performing a laboratory simulation that shows the evolution of damage to relate it to the service life of the material.

However, what is slamming? It is an impact that vessels known as speedboats experience when cruising at speeds that causes the bow to lift due to hydrodynamic lift and then fall, striking the bottom of the ship against the free water surface. The wind and sea conditions increase this problem by converting the impacts into pressure peaks that have a very short duration and, in some cases, cause catastrophic damage to ships sailing under these conditions [1-2].

Peer-review under responsibility of the Organizing Committee of DRaF2016
doi:10.1016/j.proeng.2016.11.695

In Figure 3, three moments of navigation of the SB "Bite Me" are shown [3]; these were observed during a sea trial to determine its behavior in the slamming impact produced by the planing condition of the vessel. The phenomenon of slamming consists of three clearly identified moments: in a), the vessel is gaining hydrodynamic lift; then, in b), it reaches the critical point at which the bow rises. Breaking the equilibrium, it falls, hitting the sea with the bottom of the hull, over times equivalent to microseconds, thereby generating a high pressure of slamming [4-5].

Figure 1. Navigation of the boat “Bite Me”

The rules of the classification societies such as the American Bureau of Shipping (ABS) [6] for planing boats particularly emphasize that the magnitude of the slamming pressure is directly related to the deadrise or lateral angle of the bottom of the ship with the water surface. To date, the responses to this phenomenon and its influence on the structure of vessels have not been very clearly provided, and there is much investigation. Models are studied from sections of ships to complete ship models that attempt to simulate the real scale of the effect of slamming on the boat [7-8]. To this, we must add computer models and long-term simulations that attempt to explain the harm caused by the blow pressure on the material of the ship and its premature aging. Kvålsvold and Faltinsen [9] present the results of drop tests of a plate on the crest of a wave. The results are compared with a two-dimensional theory using a beam model for the plate with impact times of less than 0.008 seconds and nonlinear beam dynamics developed by Zhao and Faltinsen [10]. Regarding the problem of simulating the short time of the peak pressure acting on the bottom of the ship, Lewis [11] and Faltinsen [12] present experimental and theoretical results that give a good idea of the times and the pressures involved in the slamming phenomenon that impact the bottom of a planing vessel. Similar results have been presented by Hermundstad et al. [13], Lavroff et al. [14], and Drummen et al. [15] and for a beam in continuous bending such as in experiments by McTaggart et al. [16], Dessi et al. [17], and Iijima et al. [18]. None of them relates the slamming phenomenon to the residual strength and energy absorption within the structure.

In the case of GFRP vessels, slamming is unique in that the impact of the sea is converted into energy that is dissipated in a composite material, producing different levels of damage, which makes studying it very complex. This phenomenon has become one of the most important in ship design directly affecting the cost, capacity, and comfort [19-21]. The structure of the boat when composed of a laminate relates to the energy dissipation in the GFRP [22]. The stresses and strains on the laminate are not uniform and vary in the direction of the surface, transversely jumping between layers and depending on the type of compound and its stresses, thereby making such damage unpredictable [23-24]. Within layers, the slamming pressure in the first instance causes the matrix to randomly rupture at and then produces delaminations between layers, which, with the increasing deformation of the panel, are joined by cracks in the matrix and form continuous steps.

This experimental approach shows a procedure to explain and predict the generation and evolution of damage in GFRP composite materials composed of preimpregnated (prepreg) sheets with Out-of-Autoclave (OoA) curing, generating peak slamming pressures in a localized manner on a specimen that occur during impact of the ship with the water surface.

The use of new OoA prepreg materials for the oven curing of GFRP structures requires special consideration in the study of energy dissipation from the slamming impact. Prepregs, as the name suggests, come in an almost inert phase, are sticky to the touch, and are dried or cured in an oven [25-29].

The procedure uses a machine designed to produce cyclic loading at different pressures close to the millisecond duration that characterize this slamming phenomenon. The stresses and strains are produced by the work of a cam, which induces the impact and deformation of a specimen. The intensity of the blow is controlled, allowing dynamic observation of the evolution of the damage, which is caused by the action of the cam on intralaminar and interlaminar defects in the composite. This stroke of the cam, which resembles the entry of water under the bottom of the ship, leaves residual damage in the tested panels because the continuous wave pressure peak accumulates damage in the material at the microstructural level. The equipment allows the frequency of impact and the strain levels applied to be varied for the purpose of using a finite element model to calculate the pressure applied by the cam in accordance with the contact area.

To integrate all information obtained experimentally and to use it in the design of new vessels, it is necessary to propose damage models to characterize the behavior of the material. A review of this subject can be found in Liu and Zheng [30] and Zhou [31]. Failure modes that occur in the material are the causes of modes in which delamination and loss of stiffness occur. [32-34]. The delamination or separation of the individual layers is an important defect that does not allow a structurally solid laminate to be maintained. Because the interlaminar toughness of laminates is the lowest, a crack spreads easily under tensile stresses at the interface. Delaminations affect the mechanical performance of the material in compression [35-36].

2. ERIMENTAL METHOD

The slamming-impact simulation machine consists of a motor with an electric variator that allows it to operate in the range of 200-320 RPM. The assembly is coupled to a shaft seated on two bearings, in between which is placed the cam that simulates the impact. This cam has previously been balanced by lightening holes to prevent unwanted inertial loads and vibrations. The cam breaks have rubber gaskets as springs to dissipate energy on the drive shaft assembly. In addition, a cycle counter is added, and there must be an optical speed reader to control the impact frequency in the tests.

All equipment is mounted within a base with two sides, top and bottom, which are used to adjust the panel to be tested, which is mounted on a frame in which it is embedded on all sides, and via top and bottom guides, it moves toward or away from the impact cam to vary the applied pressure. The eccentric shape of the cam regulated the adjustment of the panel as shown in Figure 2, allowing different values of unit deformations to be applied during the test with a contact area of 825 mm2.

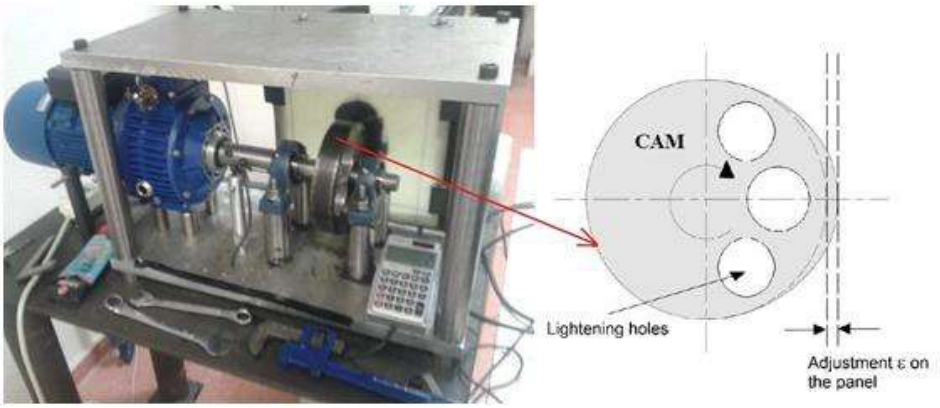

Figure 2. Slamming simulation apparatus

For the slamming test, OoA prepreg GFRP panels were prepared and stored at -18°C. Before use, they should be kept in a plastic bag that does not absorb humidity for 24 hours. The laminate was cut with fabrics of 270 x 270 mm, corresponding to dimensions of the frame of the slamming test apparatus. This included peel ply at the ends, a breathing fabric at the top, an impermeable sheet so that the resin flows to the sides and the vacuum valve is not covered, and cork bars on all four edges, with all of this tucked inside a vacuum bag. It was necessary to prove that the vacuum was maintained without leaks to ensure that during oven curing, there is a good vacuum.

The furnace employed made it possible to introduce a vacuum hose and keep the vacuum pump turned on during the curing process. The applied temperature ramp consisted of a temperature rise at 6°C per minute to 120°C, which was maintained for 90 minutes and then allowed to cool to room temperature. Figure 3 shows a panel ready for curing. After demolding, the strain gauge was placed on one side for the purpose of controlling the ε that was applied in the tests. This gauge was located at a distance of 40 mm from the center of the panel to avoid being hit by the cam.

Figure 3. Panel ready for curing

An ultrasonic inspection of each of the specimens manufactured was necessary to assess their level of porosity. To that end, an instrument called an "Automatic Ultrasonic-Immersion Inspection System" was used; it features an immersion tub for the specimens manufactured by Tecnitest and a motorized head with a reader with a scan precision of 0.1 to 0.2 mm to be used at a maximum inspection speed of 100 mm/sec, all connected to a MasterScan 335 integrated data acquisition and management instrument. This characterization made it possible to measure the percentage of defects for subsequent comparison as the material deteriorates during the slamming tests.

Specimens 15 mm wide by 250 mm long were cut for bending in three-point bending tests to determine the damage threshold of the manufactured laminate and to calculate the strain at which the material ceases to behave elastically and begins to absorb damage.

To calculate the range of pressures exerted by the cam in the contact zone, a finite element model with SOLSH190-type solid elements of eight nodes was used to simulate the laminate. This model was considered recessed at its ends and was modeled according to the dimensions of the panels. Note that the element type used is for thin structures and that the load was applied on the surface in the y-direction, with the XZ plane considered as the orientation of the laminate. According to the value obtained in strain gauges during the slamming tests, the pressures applied on the panel were estimated.

The methodology required, for the analysis of results, the residual strength of the damaged panels to be determined, for which the Airbus AITM-0010 tool was built, as presented in Figure 4. The panels

impacted by dropping weight by gravity at different ε values were tested with the tool. It is noteworthy that during the tests, the samples remained embedded on four sides to prevent the panel from tilting and erroneous data being obtained.

Figure 4. Airbus AITM-0010 compression tool after impact

The impact tests were performed on GFRP, taking advantage of the maximum performance of the apparatus in terms of the speed that could be demanded of the motor-variator set-up. Upon starting the tests, it was important not to let the cam touch the panel so that the engine could overcome the initial inertia and rotate while hitting the panel normally. During the various tests, due to friction between the cam and the panel, lithium grease was applied to reduce friction. The cam was heated, transmitting that temperature to the panel. Furthermore, the more strain applied to the panel, the more severe was the heating and the more difficult it was to overcome the initial inertia; thus, a frequency no greater than 310 RPM was used. A portable air conditioner was used to cool the paper, in addition to wet compresses applied on the opposite side of the cam to quickly lower the temperature. The temperature during the experiment was checked with a portable infrared thermography to ensure that at no point was the glass transition temperature (Tg) exceeded in the polymer matrix.

During the test, each panel was demounted between slamming-impact blocks to check the damage with ultrasound. The level of damage introduced by each slamming impact block was quantified using image analysis software (ImageJ) that allowed the number of pixels corresponding to each level of ultrasonic attenuation to be counted. The damage was also quantified by converting the color spectrum, yielding an image obtained from the ultrasound equipment in black and white, to separate the bits greater than 18 decibels that represent damage.

To analyze the type of damage within the matrix of the panels, scanning electron microscopy (SEM) was performed on one layer extracted from specimens of the low-cycle impact area and on two layers cut from the high-cycle specimens of dimensions 10 x 10 mm.

To determine how the interlaminar and interlaminar damage had expanded, the specimens were characterized by the exposure of cross sections to UV radiation. A hole was made with a 0.5 mm drill bit in the impact area, with the aim of soaking it in fluorescent penetrating liquid. Finally, these samples were exposed to UV to conduct microphotography and to observe the delamination and fracture of the matrix by making sectional cuts.

3. Results

From the test results of the three-point bending to determine the damage threshold of the laminate, by plotting ε versus δ, the results show that for values above 2314 μm/m, the laminate stops behaving elastically and begins to behave plastically. This finding indicates that there has been damage to the laminate, and therefore, this value is considered the threshold for material damage. Using the finite element model (FEM), a force equivalent to the micro-damage threshold was applied, and it was found that the pressure applied by the cam is 358 kN/m^2. Furthermore, we calculated the strain that occurs at the maximum adjustment of the panel against the cam, which corresponded to 2050 μm/m, measured with the strain gauge, upon placing a panel and applying to it the maximum impact allowed by the apparatus. This strain, calculated using the FEM, corresponded to a value of 5350 μm/m for a cam pressure of 820 kN/m^2. This result served to define the workspace of pressures and deformations in which the various tests were performed with the panels.

Compression tests were performed after impact for five test pieces that had been impacted to different ε values: 0 (non-impacted), 1921, 3394, 3750, and 4336 μm/m. The flexibility of the material, which had changed from 7000 mm/N to 12,300 mm/N, was calculated.

The selection of working pressures was made by taking a value lower than the damage threshold up to a value close to the maximum allowed by the apparatus. Table 1 shows the parameters measured in the tests.

Panel #	Pressure applied to the panel (kN/m^2)	Strain measured by strain gauge (μm/m)	Estimate strain in the center of the panel (μm/m)	Frequency (RPM)	Cycles	Load-application time per cycle (msec)	Groups of test cycles x amount executed	Number of tests conducted in ultrasound tests
A	263	650	1659	211	210,020	51.68	10,000 x 6 30,000 x 3 20,000 x 1 40,020 x 1	11
B	404	1000	2660	219	150,018	66.10	10,003 x 6 30,000 x 3	9
C	633	1570	4800	222	181,916	68.33	5000 x 10 10,000 x 4 40,440 x 1 51,476 x 1	16
D	812	2000	5250	310	21,608	71	7516 x 1 2100 x 1 2950 x 1 4042 x 1 5000 x 1	2
E	833	2050	5340	309	21,000	68.43	3000 x 3 6000 x 2	2

Table 1. Experimental variables used in the slamming tests

Panel A, which was tested with the pressure below the damage threshold value, was unchanged until 1.5 x 10^5 cycles, after which the appearance of microcracks was observed in the pressure zone of the cam. At the end of the test, at 2.1 x 10^5 cycles, the damage in the contact area came to represent 15% of the

surface. The microcracks took the orientation of the penultimate layer of the tension side (-45°), aligning and separating the fibers of this layer. Damage was observed in the last layer on the same side corresponding to the traction face. The heating of the cam and of the plate during the test was controllable and remained on the order of 55°C. For panel B, which was tested with a pressure of 404 kN/m^2, damage was obtained corresponding to 30% of the contact surface at 1.5 x 10^5 cycles. For panel C, shown in Figure 5, it was found that the microcracks grouped together randomly in the center of the contact zone and took the orientation of the penultimate layer of the tension side (-45°) at 1.8 x 10^5 cycles, with 25% damage in the area in contact with the cam and an average temperature of 70°C during the test

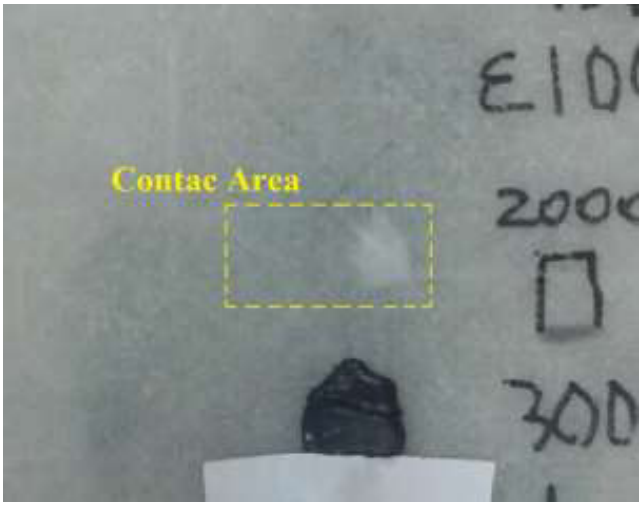

Figure 5. Damage to panel C at 1.8 x 10^5 cycles of impact at P = 633 kN/mm^2

Of the samples taken from panel C, the following was observed with SEM, as shown in Figure 6. In image a), interlaminar porosity that has resulted in delamination due to low-energy impact is observed. Image b) shows a number of interlaminar pores that are linked with each other to form a continuous delamination in some areas under the action of repeated impacts, which simulate slamming. Image c) shows the detail of a pore with fibers aligned under a thin film of polymer. At this same site, image d) reveals the cross section of three fibers that appear outside the polymer matrix, indicating that there is good adhesion at the fiber-matrix interface.

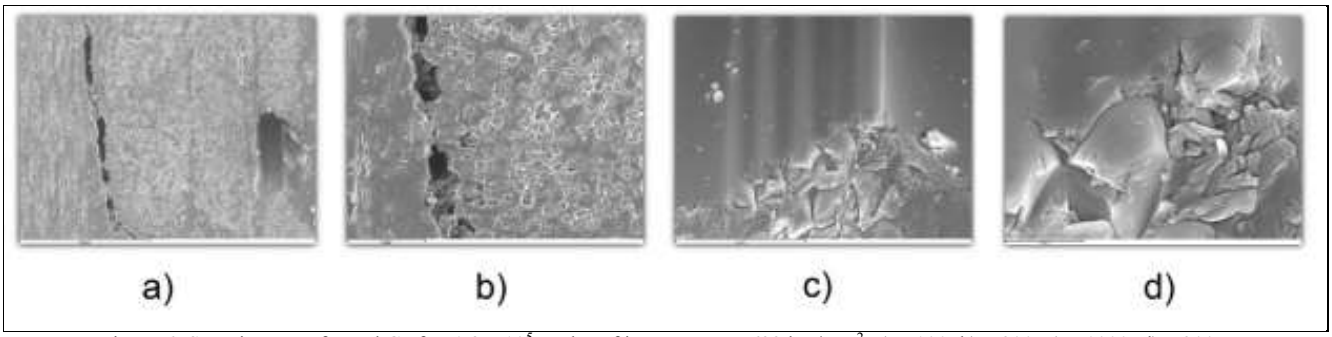

Figure 6. SEM images of panel C after 1.8 x 10^5 cycles of impact at P = 633 kN/mm^2. a) x 100, b) x 300, c) x 1000, d) x 300

For panels D and E, in which the maximum pressure corresponding to 812 and 833 kN/m^2, respectively, was applied, blocks of cycles applied in each test could not be regular because the temperature rose too quickly. It reached the order of 70°C, and the cooling methods were no longer sufficient to prevent a temperature rise. The steel cam maintained much residual heat in its mass, and testing had to stop until the cam reached room temperature. It

was observed in the panels that this friction wore the laminate surface resin despite the lithium grease applied, but when the cam touched the fiber, wear no longer occurred. The temperature rise gradient varied from 3° to 10° per minute. The application of cold wet cloths lowered the panel temperature on the order of 20°C instantly and made it possible to test the panel for more cycles without stopping the slamming equipment. These panels had greater damage in a low number of cycles on the order of 2.0 x 10^4. Microscopy of panel D indicates that additional plastic flow occurred in the polymer matrix as an effect of the temperature, as shown in Figure 7.

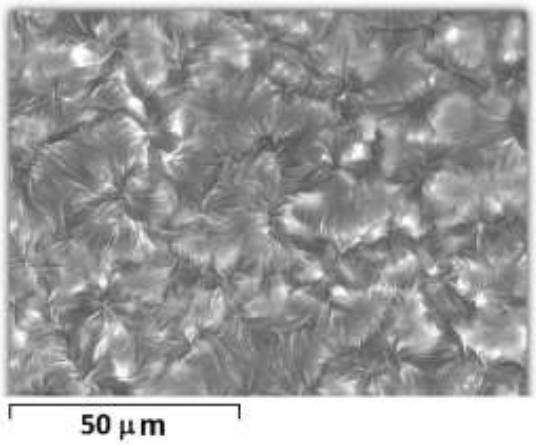

Figure 7. SEM image of panel D after 2.1 x 10^4 cycles of impact at P = 812 kN/mm^2

Panel E reached 88% damage in the area of contact with the cam at the end of the 2.1 x 10^4 impact cycles. Figure 8 shows the evolution of damage in the area of contact with the cam, which has been plotted because the percentage of area damaged in this zone varies, versus applied slamming cycle. The material quickly shows microcracks at 2000 impacts in a focused area; they grow in a circular shape that expands until, at 5000 cycles, a shadow appears in another part of the contact zone, indicating that the microcracks have increased in number. Hence, the material exhibits rapid damage up to near 1.1 x 10^4 cycles, at which point the final degradation of the material begins to expand over the entire contact area.

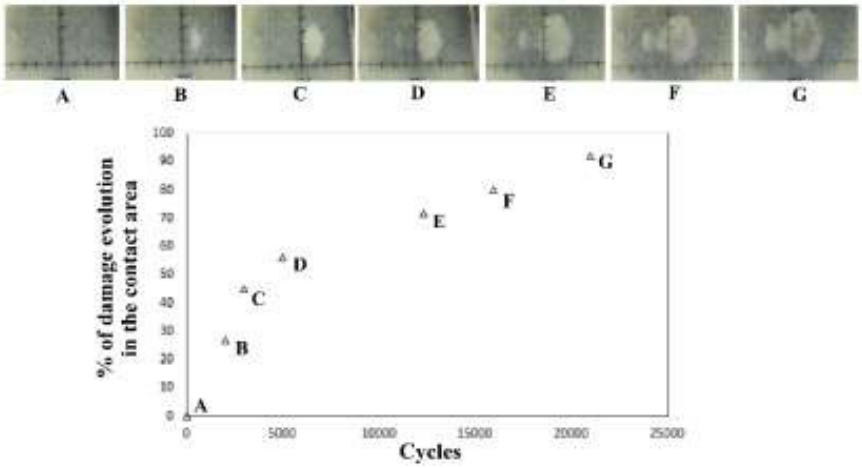

Figure 8. Damage evolution of panel E until 2.1 x 10^4 cycles of impacts at P = 833 kN/m^2

Ultrasound analysis on each panel between impact blocks was performed on an equivalent 150 x 150 mm surface, taking the impact zone as the center. A comparison of the percentage of damaged parts from panel C without impacting and impacted at a pressure of 633 kN/m^2 is shown in Figure 9. Ultrasound analysis was conducted on the panel without impacting, and a color image, which was then converted into black and white, was

obtained. The percentage of damage obtained was 2.05%. At the end of the test, the same procedure was applied to the end of the impact cycle block with 1.8 x 10^5 accumulated cycles, which resulted in 5.80% damaged parts in the panel.

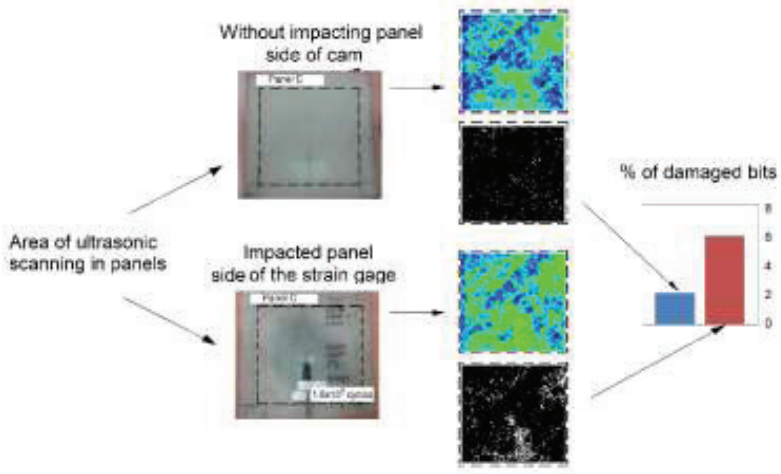

Figure 9. Ultrasound comparison of panel C without impacting and after 1.8 x 10^5 cycles of impact at P = 633 kN/m^2

Figure 10 shows the level of damage of the panels impacted by slamming versus the number of impacts received for each of the ultrasound tests. It is noted that panels A, B, and C in the regimen of progressive damage at high numbers of cycles do not exceed 6% damaged parts. For panel D, although it is part of the regime of low-cycle progression, the ultrasound testing is not representative for the point damage received in the area in contact with the cam in relation to the total swept area, as is the case with panel E.

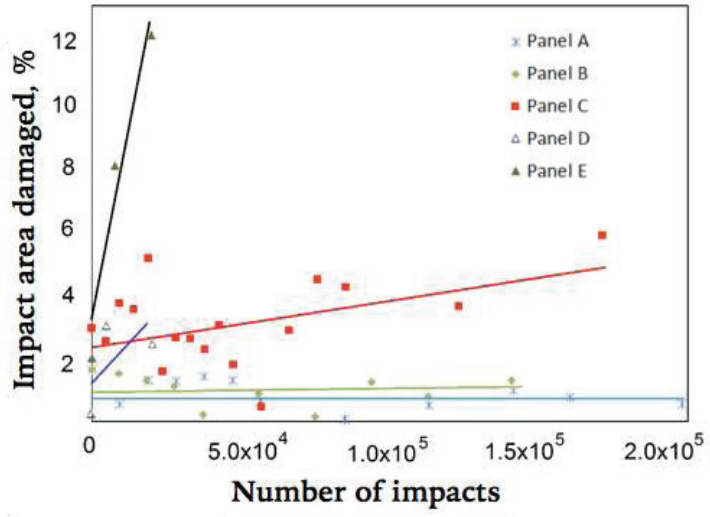

Figure 10. Comparison of percentage of damaged area

According to the damage-percentage ratio for the total cycles per panel tested at different pressures, Figure 11 shows the trend in damage obtained with the slamming apparatus. For pressures greater than 700 kN/mm^2 damage per cycle imposed on the material, there is a low-cycle damage progression regime, on the order of 10^4 slamming impact strokes. For pressures less than this value, the tests are in the low-cycle damage progression regime, or on the order of 10^5 strokes.

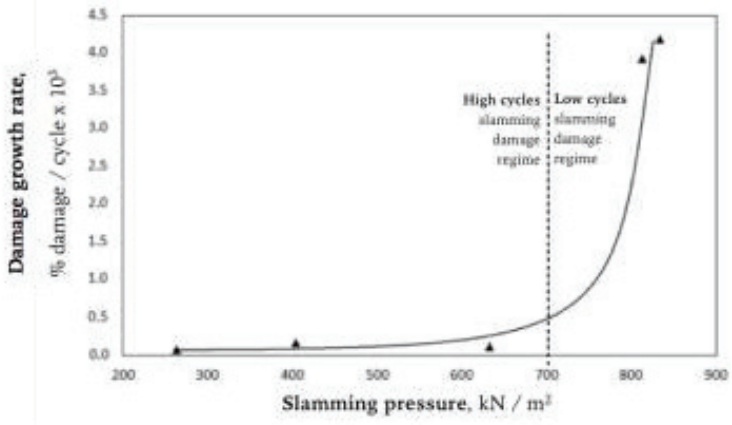

Figure 11. Percentage of damage/cycle with the pressures applied on the panels

Based on the UV characterization tests, it was observed that the damage of the panels exhibited vertical fractures, which corresponded to the damage in the matrix, in addition to delaminations that linked together in staggered fashion between each of the layers. Figure 12 shows an impacted panel equivalent to a slamming pressure of 830 kN/m^2.

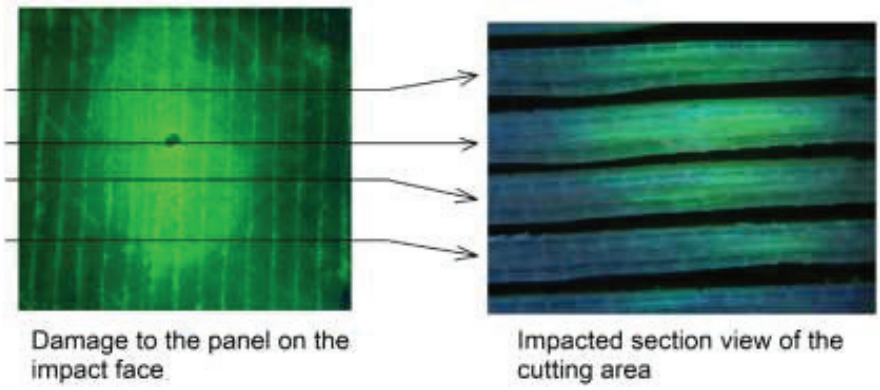

Figure 12. Cross sections of a panel impacted at 40 joules

4. Discussion

The methodology and apparatus used have made it possible to simulate the slamming impact on a composite panel and dynamically observe the evolution of damage in an OoA-type GFRP laminate under the applied conditions of pressure, strain, and impact frequency. This type of OoA material employs a lighter matrix that partly sacrifices rigidity, which is a condition that is directly related to the phenomenon of slamming.

Based on the experimental results, several internal failure modes could be predicted within the composite laminate from the perspective of micromechanics, which made it possible to predict the onset of mesocracks, microcracking in the matrix, fiber debonding, fiber removal, and delamination. Under a compressive load along the fiber direction, a fracture mode transverse to the tension was observed in which the strain exceeds the deformability of the composite material in the form of microbuckling and shear through the fibers when the composite is loaded in the direction perpendicular to the fiber orientation. In the tests, the breaking of fibers during the application of load on the composite has been the defining behavior at critical stress and induces a redistribution of stress, exerting an influence on the evolution of the cracks. This phenomenon is the fundamental basis of what is observed in the

simulation and of how damage has accumulated in each of the layers. In addition, observing the anisotropic behavior, the directional dependence of the state of stresses allows the microcracks to couple perpendicularly between the 45° layers by creating shear stresses, for the tested panels. The relationship between the slamming pressure on the composite and the percentage of damage per cycle has an abrupt increase in intensity over a certain pressure value. The reason is that microcracks that rapidly align with higher stress fibers are oriented to reach fracture through the decrease in the rigidity and the increase in the fragility of the prepreg.

Failure prediction models using micromechanical composite materials can provide a locally accurate description of the failure initiation at critical points. Microscopy has shown that the equipment makes it possible to differentiate damage that goes from interlaminar to intralaminar and measure the degradation of stiffness with the application of loading cycles and the rupture of the laminate at pressures less than the static limit, which are always related to plastic deformation according to the results. The microstructure observed for low-cycle testing and the temperature increase produced by the dissipation of stresses in the material cannot be estimated because the friction from the cam during the tests raises the temperature over this level, given that the slamming simulation apparatus is not adiabatic. Delamination is considered one of the critical failure mechanisms that can substantially reduce the residual strength of the composite plate, particularly under compression.

At this level of pressure, with the change in the per-cycle damage percentage, the slamming apparatus allows the dynamics of the redistribution of stress to be physically observed and the presence of discontinuities to be explained. In this manner, the tests went from low-energy slamming impact, in which microcracks are aligning in an interlaminar form, to medium energy impacts, in which the interlaminar damage also produces intralaminar damage, which was confirmed by SEM.

Monitoring the damage with ultrasound analysis and imaging makes it possible to quantify the increase in microcracks and to assess the level of damage to the panels after the cyclical impacts. Using ultrasound, it is clear that the apparatus does not produce a direct delamination phenomenon because the slamming pressure level generates microfractures in the matrix that are directly related to the service life of the composite and, therefore, its residual strength. The restricted compression test confirmed and clearly presented how the material has changed the residual strength of the laminate after impact, and the type of damage can be linked to the non-linear irreversible stress that the damage in a composite material produces, which depends on the effective damage stress in its main orthotropic components. The SEM observation of the matrix made clear that the temperature influenced delamination because, during the appearance of residual stresses, the composite melted again, thereby increasing intralaminar resistance.

The UV characterization of the panels allows the damage done to the matrix and the delaminations that occur to be visualized, and these results can be processed to produce 3D images of the panel layers.

This study definitively makes it possible to evaluate the lifetime of the impacted material in the hull of a planing vessel and to predict the cumulative stress that would make the vessel unusable.

Acknowledgements

The authors would like to thank the Madrid Polytechnic University (Universidad Politécnica de Madrid, UPM) for the Project RP150831009. They would also like to express their gratitude to the laboratory technical staff: Ms. Ana Soria and Ms. Ana García.

References

1. K. Sungeun, D. Novak., "Slamming impact design loads on large high speed naval craft". SuperFAST'2008, July 2-4, 2008, Saint-Petersburg, Russia.

2. DNV, "Environmental condition and environmental loads". Recommended Practice DNV-RP-C205, Octubre 2001.

3. LP Bite Me, 12,40 m de eslora, Registro Puerto Ayora, Ecuador. Año de construcción 2010.

4. McCue L., "Statistics and Design Implications of Extreme Peak Vertical Accelerations from Slamming of Small Craft". SNAME. 2012.

5. Bloundt D, Codega L, "Dinamic Stability of Planning boat". SNAME. 1992.

6. ABS, "Rules for Building and Classing High-Speed Craft". American Bureau of shipping, Parte 3, chapter 2, sección 2. 2015. Pág 61-65.

7. B. G. Kabsenberg, "Slamming or ships: where are we Now?". Philosofical Transactions of Royal Society, 20 de junio de 2011. Pág 2892-2897.

8. Kapsenberg, G. K., Veer, A. P., "Whipping loads due to aft body slamming". 24th Symposium. on Naval Hydrodynamics, Fukuoka, Japan, July 2002.

9. Kvalsvold J., Faltinsen O., "Slamming loads on wetdecks of multihull vessels". International Conferenece on Hydroelasticiy in Marine Technology, Norway 119.

10. Zhao R., Faltinsen O., "Water entry of 2-dimensional bodies". J. Fluid Mechanical 246, 593-612.

11. Lewis, S. G., Hudson, D. "Impact of a free-falling wedge with water: synchronized visualization, pressure and acceleration measurements". Fluid Dyn. Res. 42, 1–30. (doi:10.1088/0169-5983/42/3/035509) 2010.

12. Faltinsen O., "Slamming". Proc. Colloquium for ship and Offshore Hydrodinamics, Report no. 561 Germany. 1996.

13. Hermundstad O., Aarsnes J., "Hydroelastic analysis of a flexible catamaran and comparison with experiments". FAST. Germany 1995.

14. Lavroff J., Davis, M., "The whipping vibratory response of a hydroelastic segmented catamaran model". FAST, China. 2007.

15. Drummen I., Storhaug G., "Experimental and numerical investigation of fatigue damage due to wave-induced vibrations in a container ship in head seas". Journal of Maritime Science Technological. 13, 428-445.

16. McTaggart K., Datta I., "Motions and loads of a hydroelastic frigate model in severe seas". SNAME Annual Meeting. Canada. 1997.

17. Dessi D., Mariani R., "Experimental analysis of the wave induce response of a fast monohull via segmented-hull model". FAST Italy. 2003.

18. Iijima K., Hermundstad O., "Symmetric and antisymmetric vibrations of a hydroelastically scaled model" 5th international conferencia on Hydroelasticity in Marine Technology". Norway. 1994.

19. Hayman B., "Response of sandwich structures to slamming and impact loads". Composite Materials in Marine Structures, vol. 2. Cambridge University Press, Cambridge, Great Britain (Chapter 9). 1993.

20. Z. Qin, R.C. Batra, "Local slamming impact of sandwich composite hulls", International Journal of Solids an Structures 46 (2009) 2011-2035.

21. Chen JK, Sun CT., "Dynamic large deflection response of composite laminates subjected to impact". Compos Struct 4:59e73. 1985

22. S. Lake, M. Eagle "Slamming of Composite Yacht Hull Panels". The 18th Chesapeake Sailing Yacht Symposium. Marylan 2007.

23. Pedro Tamayo-Meza1, Anatoly S. Ovchinsky, "Estudio de la Dinámica de los Procesos de Fractura y de Delaminación en Materiales Reforzados con Fibras". Revista de la Facultad de Ingenieria de la Universidad de Antioquia N. º70 pp. 119-131, marzo, 2014.

24. A. Turon a, J. Costa a, "Simulation of delamination in composites under high-cycle fatigue". AMADE, Spain November 2006. Pág 1.

25. Umeco, "Advanced composites and process materials for the marine industry". Umeco industry research. Extraído el 6 de Noviembre de 2012,

26. James K. Sutter1, W. Scott Kenner2, “Comparison of Autoclave and Out-of-Autoclave Composites”. NASA Glenn Research Center, Cleveland, OH. 44135. Extraído el 1 de Noviembre de 2012

27. Hubert P., “Aspects Of Flow And Compaction Of Laminated Composite Shapes During Cure”. Thesis submitted in partial fulfillment of the requirements for the degree of Doctor of, Department of Metals and Materials Engineering. the University of British Columbia July 1996.

28. Shim VPW, Yang LM.,” Characterization of the residual mechanical properties of woven fabric reinforced composites after low-velocity impact”. Int J Mech Sci 47:647e65. 2005

29. Hou T., “A theoreticalstudy of resin flows for thermosetting materials during prepreg processing”. Nasa Contractor Report, USA. Julio 1984.

30. P.F. Liu, Y. Zheng, “Recent developments on damage modeling and finite element analysis for composite laminates: A review”, Materials and Design 31 (2010) 3825-3834.

31. Zhou G. “The use of experimentally-determined impact force as a damage measure in impact damage resistance and tolerance of composite structures”. Composite Structural 42:375e82. 1988

32. Brien TK. Analysis of local delaminations and their in¯uence on composite laminate behaviour. Delaminations and debonding of materials. ASTM STP 876 W.S. Jhonson ASTM 1985.

33. Lopes C., Seresta O., “Low-velocity impact damage on disperse stacking secuence laminates. Part I: experiments”. Compos Sci Tenchol 69(2009) 926-936

34. Shi Y., Swait T, “Modelling damage evolution in composite laminates subjected to low velocity impact”. Composite Structures 94 (2012) 2902–2913

35. Lopes C., Cammanho P., “Low-velocity impact damage on dispersed stacking sequence laminates. Part II: Numerical simulations”. Composites Science and Technology 69 (2009) 937–947

36. Raimondo L. , Lannuci L., “A progressive failure model for mesh-size-independent FE analysis of composite laminates subject to low-velocity impact damage”. Composites Science and Technology 72 (2012) 624–632